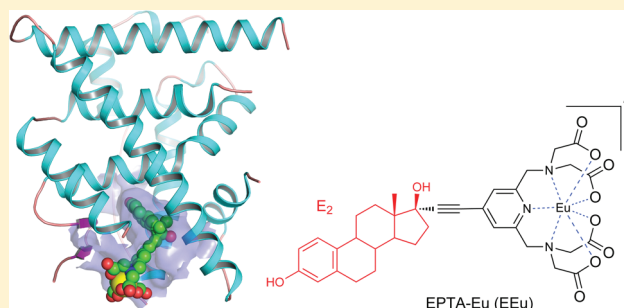


# Structure of Estradiol Metal Chelate and Estrogen Receptor Complex: The Basis for Designing a New Class of Selective Estrogen Receptor Modulators

Min-Jun Li,<sup>†,‡</sup> Harry M. Greenblatt,<sup>†</sup> Orly Dym,<sup>§</sup> Shira Albeck,<sup>§</sup> Adi Pais,<sup>‡</sup> Chidambaram Gunanathan,<sup>||</sup> David Milstein,<sup>||</sup> Hadassa Degani,<sup>‡</sup> and Joel L. Sussman<sup>\*,†,§</sup>

<sup>†</sup>Department of Structural Biology, <sup>‡</sup>Department of Biological Regulation, <sup>§</sup>Israel Structural Proteomics Center (ISPC), and <sup>||</sup>Department of Organic Chemistry, Weizmann Institute of Science, Rehovot 76100, Israel

**ABSTRACT:** Selective estrogen receptor modulators, such as 17 $\beta$ -estradiol derivatives bound to metal complexes, have been synthesized as targeted probes for the diagnosis and treatment of breast cancer. Here, we report the detailed 3D structure of estrogen receptor  $\alpha$  ligand-binding domain (ER $\alpha$ -LBD) bound with a novel estradiol-derived metal complex, estradiol-pyridine tetra acetate europium(III), at 2.6 Å resolution. This structure provides important information pertinent to the design of novel functional ER $\alpha$  targeted probes for clinical applications.



## INTRODUCTION

Estrogens and their main targets, estrogen receptors (ER $\alpha$  and ER $\beta$ ), play key roles not only in the maintenance of normal sexual and reproductive function but also in the progression of numerous diseases.<sup>1,2</sup> In ER-positive breast cancers, estrogen-receptor  $\alpha$  (ER $\alpha$ ) is the major and well-established biomarker for the assessment of prognosis and for predicting the response to endocrine therapy with selective estrogen receptor modulators (SERMs) and selective estrogen receptor down-regulators (SERDs),<sup>3</sup> such as hydroxytamoxifen (Figure 1). A series of estrogen-derived metal complexes have been designed as targeting drugs to deliver special functional units into ER-positive cells, which in turn may be used for chemotherapy,<sup>4</sup> as well as diagnostic imaging purposes, viz., targeted MRI contrast reagents.<sup>5</sup> The design and synthesis of a new series of SERMs, composed of lanthanide (Ln) chelates of estradiol-pyridine tetra acetate (EPTA-Ln), was recently reported.<sup>5</sup> The Ln can be any of the lanthanide ions, such as Gd<sup>3+</sup> or Eu<sup>3+</sup> (Figure 1). Taking advantage of the paramagnetic properties of lanthanide ions and, in particular, Gd<sup>3+</sup>, EPTA-Gd can be used as a contrast reagent in MRI studies of target organs and tissues responsive to estrogens.<sup>5</sup> These new SERMs show binding affinities to ER $\alpha$  in the range of 1  $\mu$ M (employing a competitive radiometric binding assay with titrated 17 $\beta$ -estradiol, E2).<sup>5</sup> One might assume that the presence of a large bulky side chain attachment in EPTA-Ln molecules would give rise to antagonistic behavior as with other ER antagonists (Figure 1). However, because of the attachment position being C17 (Figure 1, estradiol-pyridine tetra acetate europium, EPTA-Eu) rather than C7 (Figure 1, SERDs)<sup>6</sup> of the steroid core, EPTA-Ln molecules exhibit agonist behavior similar to that of E2, stimulating

cell proliferation and inducing ER $\alpha$  degradation in ER-positive breast cancer cells.<sup>5</sup>

It was previously shown that it is possible to append a bulky organometallic moiety at the 17 $\alpha$ -position of estradiol, while maintaining both affinity for the ER<sup>5,7</sup> and estrogenic behavior.<sup>5,8</sup> Recently, lanthanide chelates of progesterone, specifically targeted to the progesterone receptor and applied as contrast agents, have also been reported.<sup>9</sup> However, the molecular mechanisms underlying the interaction of such ligands with the receptor and the ensuing biological activity are not known. Here, we report a novel conformation of the ER $\alpha$  ligand-binding domain (ER $\alpha$ -LBD), complexed with EPTA-Eu, at 2.6 Å resolution. This crystal structure provides a molecular basis for understanding the estrogenic–agonistic activity of this type of ligand.

Many crystal structures of complexes of ER-LBDs with SERMs have been determined.<sup>2</sup> The ER $\alpha$ -LBD structure has the same three-layer helical “sandwich” fold as found in other nuclear receptors (NRs), and its ligand occupies a buried, hydrophobic ligand-binding pocket (LBP), which is located in the lower part of the LBD.<sup>10</sup> The LBP is seen to be more flexible than the upper portion of the LBD and exhibits some of the properties of a molten globule.<sup>11</sup> The binding of E2 stabilizes this region,<sup>12</sup> especially the conformation of the C-terminal helix, helix 12 (H12). Different SERMs modulate H12 so as to generate different conformations in the surface area of the LBD.<sup>6,10,13,14</sup> The exact conformation of H12 is critical for cofactor binding and transcriptional activation of ER $\alpha$ . Therefore, most structural

Received: February 20, 2011

Published: April 07, 2011

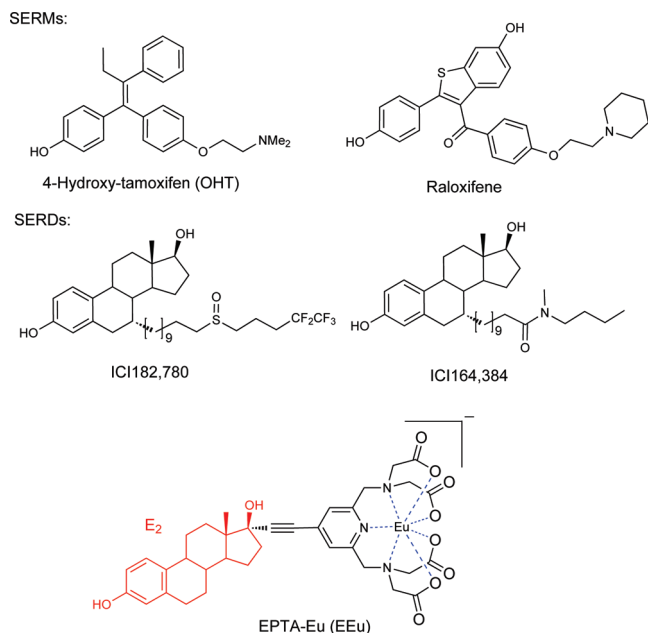


**Figure 1.** Chemical structures of representative SERMs and SERDs and of the novel Eu derivative (EPTA-Eu) developed in the present study.

studies of ER-LBDs have focused on ligand-dependent conformational changes in H12. However, structural analysis of the LBDs of both ERs and other NRs has shown that other helical and loop elements that contribute to the LBP also adopt different conformations upon binding different ligands.<sup>15</sup> Recent X-ray studies suggest that the flexibility and plasticity of the entire LBP of ERs,<sup>16</sup> and of other NRs, such as the glucocorticoid receptor (GR)<sup>17</sup> and the pregnane X receptor (PXR),<sup>18</sup> provide it with the conformational space to expand in different directions, depending on the chemical nature of the bound ligand, as indeed is shown here for the complex of ER $\alpha$ -LBD with EPTA-Eu.

On the basis of the published ER-LBD structures, it appears that the ligands are fully buried within the LBP. Because no obvious entries or exit routes have been reported, the route(s) of movement of the ligand into and out of the LBP are inferred solely on the basis of the observed orientations of H12, resulting in the so-called “mouse-trap” model. However, recently, molecular dynamic simulations were used to study escape of ligand from ER-LBD and predicted up to seven possible escape pathways.<sup>19–22</sup> These pathways are influenced by the starting structure models, e.g., monomer or dimer, and by the chemical nature of the ligand and the protein conformations that the ligand induces. In the present study, the structure of the EPTA-Eu/ER $\alpha$ -LBD complex displays an open conformation that suggests a “clamp” model of ligand binding. Overall, the structure provides a molecular basis for understanding the estrogenic–agonistic activity of this type of ligand. On the basis of this structural information, a new series of molecules with stronger paramagnetic or fluorescent effects is being developed.

## EXPERIMENTAL SECTION

**Protein Purification and Crystallization.** Although ER $\alpha$ -LBD (~28.7 kDa) has four cysteine residues (C381, C417, C447, and C530), no intramolecular disulfide bonds are found in the protein.<sup>23</sup> To avoid the formation of intermolecular disulfide bonds during expression and purification of the protein, three of the cysteine residues (C381, C417,

**Table 1.** Data Collection and Refinement Statistics

		EPTA-Eu/ER $\alpha$ LBD
PDB entry code		2YAT <sup>a</sup>
data collection		
X-ray source		ESRF beamline ID29
temperature (K)		100
wavelength (Å)		0.979
space group		P3 <sub>2</sub> 12
unit cell dimensions		
<i>a</i> , <i>b</i> , <i>c</i> (Å)		64.69, 64.69, 133.35
$\alpha$ , $\beta$ , $\gamma$ (°)		90.0, 90.0, 120.0
<i>R</i> <sub>sym</sub> <sup>c</sup> (%)		13.0 (67.2) <sup>b</sup>
<i>I</i> / $\sigma$		8.7
refinement		
resolution (Å)		50.0–2.60 (2.64–2.60) <sup>b</sup>
completeness (%)		100 (100) <sup>b</sup>
unique reflections		10,104
redundancy		19.9 (10.7) <sup>b</sup>
<i>R</i> <sub>work</sub> <sup>d</sup> / <i>R</i> <sub>free</sub>		0.183/0.229
rmsd bond lengths (Å)		0.009
rmsd bond angles (°)		2.1
no. of nonhydrogen atoms in ASU		
total		1888
protein		1811
ligand/ion		49
water		28
<i>B</i> factor (Å <sup>2</sup> )		
overall		68.1
protein		68.09
ligand/ion		75.77
water		56.20
Ramachandran plot analysis (%)		
favored		98.64
allowed		0.91
outliers		0.45

<sup>a</sup> An animated Interactive 3D Complement (I3DC) appears for 2YAT in *Proteopedia* at <http://proteopedia.org/w/Journal:JMedChem:1>. <sup>b</sup> Values in parentheses are for the highest resolution shell. <sup>c</sup>  $R_{\text{sym}} = \sum |I_i - \langle I_i \rangle| / \sum I_i$ , where  $I_i$  is the observed intensity and  $\langle I_i \rangle$  is the average intensity obtained from multiple observations of symmetry-related reflections. <sup>d</sup>  $R_{\text{work}} = \sum_{hkl} ||F_o| - |F_c|| / \sum_{hkl} |F_o|$ . Five percent of the reflections were excluded for the  $R_{\text{free}}$  calculation.

and C530) were mutated to serine. C447, which is buried inside the LBD, was not mutated. Previous publication showed that these mutations will not change the conformation of ER $\alpha$ LBD.<sup>24</sup> The triple mutant (C381S, C417S, and C530S) human ER $\alpha$ LBD (residues Ser301–Ala551) was produced using the pET21a/*Escherichia coli* BL21 (DE3) expression system and was purified on an E2-Sepharose affinity column.<sup>25</sup> The ER $\alpha$ LBD/EPTA-Eu complex was obtained by including a 150  $\mu$ M concentration of the ligand in the column elution buffer, which was 50 mM arginine–glutamic acid, 100 mM NaCl, and 50 mM HEPES, pH 7.5. Protein purified from the E2-affinity column was concentrated to 5 mg/mL and taken for crystallization without further purification. Crystals were obtained by vapor diffusion at 19 °C using the hanging-drop method. Two microliters of protein solution (5 mg/mL) was mixed with 2  $\mu$ L of reservoir solution, viz., 20% polyethylene glycol monomethyl ether 5000, 5% Tacsimate,<sup>26</sup> and 0.1 M HEPES, pH 7.0

[Tacsimate is a mixture of a particular set of organic acids supplied by Hampton Research (Aliso Viejo, CA)]. This mixture equilibrated against the reservoir solution for at least 3 weeks. Cubic crystals of dimensions  $\sim 20 \times 20 \times 100 \mu\text{m}^3$  were thus obtained. Prior to data collection, the crystals were flashed-cooled in liquid nitrogen with a cryoprotectant buffer (20% polyethylene glycol and 80% reservoir solution).

**Data Collection and Structure Determination.** X-ray diffraction data were collected at beamline ID29 at the European Synchrotron Radiation Facility (Grenoble, France). The X-ray data were processed using the HKL2000 program suite.<sup>27</sup> The structure was solved by molecular replacement using PHASER<sup>28</sup> from CCP4 package,<sup>29</sup> with the structure of ER $\alpha$ LBD<sup>16</sup> (PDB ID entry code 2P15) as the starting model. The initial  $2F_o - F_c$  and  $F_o - F_c$  electron density map clearly showed the position and shape of the EPTA-Eu ligand. The model of EPTA-Eu (EEu) was constructed using the Gaussian09 program (Gaussian, Carnegie, PA), and a parameter cif file was generated using eLBOW.<sup>30</sup>

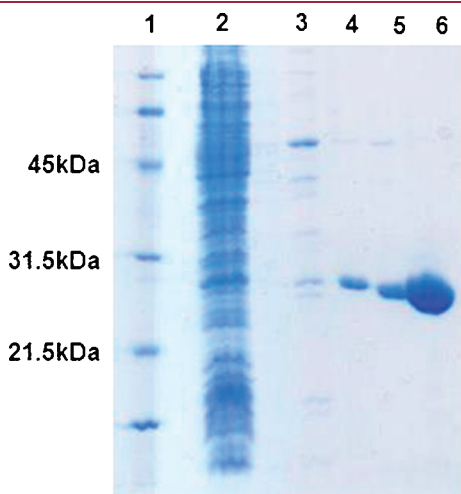


**Figure 2.** SDS-PAGE ER $\alpha$ -LBD purified on an E2-affinity column. Lane 1, low molecular weight protein markers; lane 2, flow-through from the E2-affinity column; lane 3, E2-affinity column wash; lane 4, ER $\alpha$ -LBD eluted with  $100 \mu\text{M}$  EPTA; lane 5, ER $\alpha$ -LBD eluted with  $100 \mu\text{M}$  EEu; and lane 6, ER $\alpha$ -LBD eluted with  $50 \mu\text{M}$  E2.

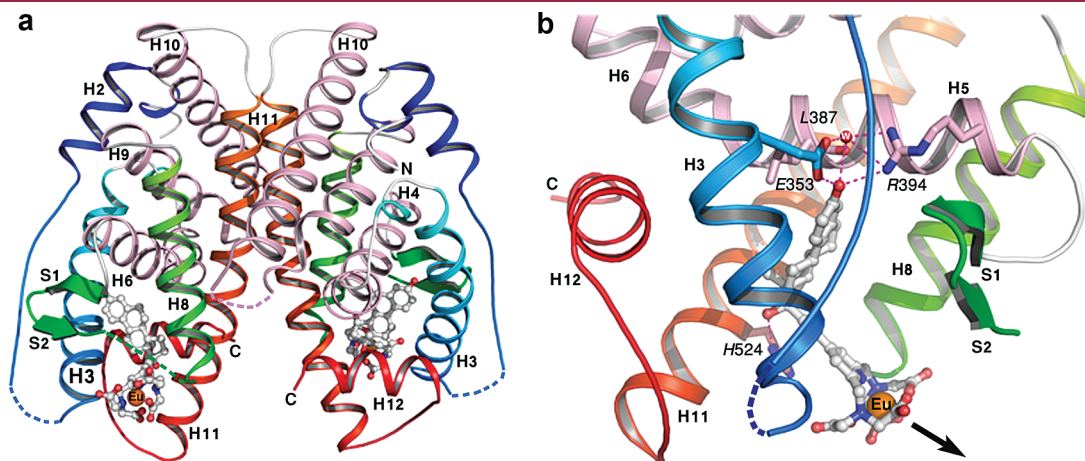


**Figure 3.** Overall crystal structure of the EEu/ER $\alpha$ -LBD complex. (a) The homodimeric structure of the complex. EEu is shown as gray balls-and-sticks, with  $\text{Eu}^{3+}$  displayed as a golden sphere. Dashed lines indicate unmodeled regions of the structure. The N and C termini, and the helices (H) and  $\beta$ -strands (S) are labeled accordingly. (b) Detailed view of the ligand-binding region of the complex, showing the orientation of EEu, with the Eu-tagged side chain pointing to an open space toward H8, and unobserved H7, as indicated by black arrow. The residues H-bonding to the ligand are displayed and labeled in italics. A water molecule, involved in the H-bond network, is shown as a red sphere, labeled W. The figure was created with PyMol, and the helices are rainbow colored from N to C direction.

Successive alternation of refinement cycles and manual model building was performed using PHENIX<sup>31</sup> and Coot<sup>32</sup> until convergence to values of  $R_{\text{work}} = 18.3\%$  and  $R_{\text{free}} = 22.9\%$ . Translation/libration/screw (TLS) refinement was performed at each refinement round. The TLS groups were determined by the TLS Motion Determination server.<sup>33</sup> The final model was validated using MOLPROBITY.<sup>34</sup> Details of data collection, processing, and structure refinement are summarized in Table 1. A simulated annealing omit map and an anomalous scattering map were calculated using PHENIX.<sup>31</sup> The final model comprises residues 301–330, 341–413, 423–461, and 464–548. The unmodeled regions correspond to residues 331–340 within the  $\omega$ -loop located between helices H2 and H3, to the disordered residues of H7 (414–417), to the loop between H7 and H8 (418–422), and to residues 462–463 in the loop joining H9 and H10.

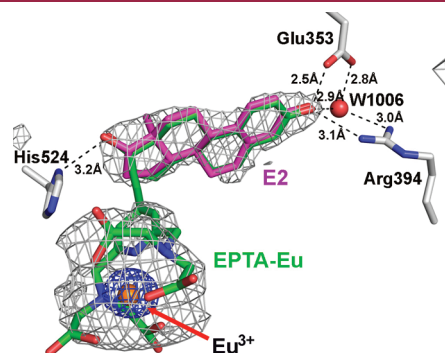


**Figure 4.** Ligand binding site of the EPTA-Eu (EEu). The  $F_o - F_c$  simulated annealing omit map of the ligand EPTA-Eu (green stick) is contoured at  $3.0\sigma$  and shown as gray mesh. The anomalous map contoured at  $20\sigma$  (blue mesh) clearly shows the  $\text{Eu}^{3+}$  ion (orange sphere) of the ligand EEu. The structure of E2 in the complex of E2/ER $\alpha$ -LBD complex (PDB ID: 1ERE<sup>10</sup>), displayed in magenta, is superimposed. It can be seen that the E2 core of EEu overlaps closely with that of E2 itself. The residues (Glu353, Arg394, and His 524) and the conserved water molecule (W1006) forming hydrogen bonds are displayed as sticks, with oxygen atoms in red and nitrogen atoms in blue. Hydrogen bonds between the LBD and the E2 moiety of ligand are shown as black dashed lines.

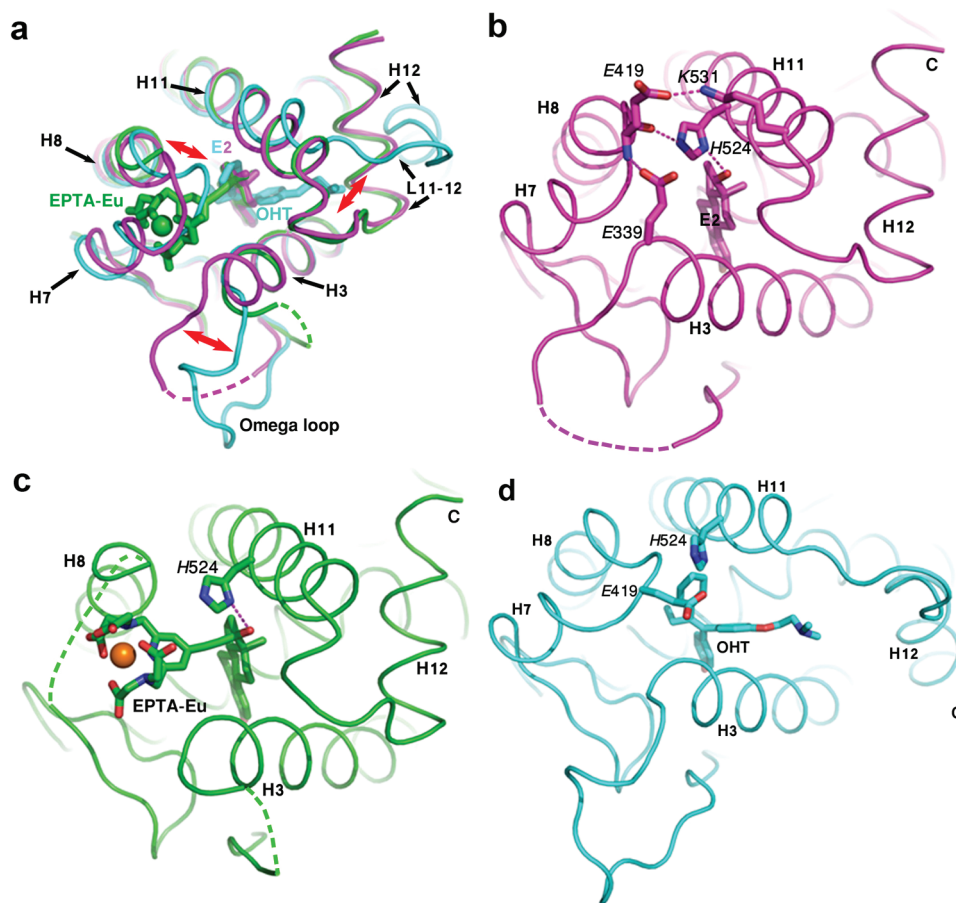


**Figure 5.** C $\alpha$  traces of the E2/ER $\alpha$ -LBD, EEu/ER $\alpha$ -LBD, and OHT/ER $\alpha$ -LBD complexes. Dashed lines indicate unmodeled regions of different structures. (a) Superimposed ribbon representations of the C $\alpha$  traces of all three complexes, E2/ER $\alpha$ -LBD (magenta, 1ERE), OHT/ER $\alpha$ -LBD (cyan, 3ERT), and EEu/ER $\alpha$ -LBD (green). The numbering of the helices (H) is the same as shown in Figure 3. Putative synergistic reciprocating movements within the LBP are shown by red arrows. (b–d) Ribbon representations of the respective individual the C $\alpha$  traces. Dashed lines indicate unmodeled regions of the C $\alpha$  traces. H-bonds between the ligands and the residues of H3, H7–H8, and H11 are shown as pink dotted lines. Residues involved in the formation of H-bonds are shown as sticks labeled with italic single letters. (b) The H-bonds made by the 17 $\beta$  hydroxyl of E2 with His524 and Lys531 of H11, Glu419 of H7, and Glu339 of H3 may work together to tighten the neck of the LBP upon binding of the endogenous ligand, E2. (c) A single H-bond is formed between the 17- $\beta$  hydroxyl of the E2 moiety of EEu. H-bonds with other residues, as seen in the E2/ER $\alpha$ -LBD complex, cannot be modeled in the EEu/ER $\alpha$ -LBD complex. (d) There are no H-bonds formed between OHT and residues in H3, H7–H8, and H11 within the OHT/ER $\alpha$ -LBD complex.

## RESULTS AND DISCUSSION

**Dimerization Pattern of ER $\alpha$ -LBD.** ER $\alpha$ -LBD/ligand complexes were purified on an E2-affinity column<sup>25</sup> using elution buffers containing E2, EPTA, or EPTA-Eu. Sodium dodecyl sulfate–polyacrylamide gel electrophoresis (SDS-PAGE) (Figure 2) showed that in all three cases the protein eluted was of high purity. The elution profile of the purified complexes upon gel filtration on a Superdex HR 10/30 column indicates a mass of ~60 kDa, corresponding to the molecular size of ER $\alpha$ -LBD dimer.

The crystal structure shows that the binding of EPTA-Eu (EEu) ligand does not affect the dimerization pattern of the protein (Figure 3a). The homodimer is formed by the 2-fold crystallographic axis (Table 1) and shows the same overall dimeric arrangement as seen in the E2/LBD complex.<sup>10</sup> Because of the orientation of the Eu<sup>3+</sup>-chelated tag on the EEu within the LBP, which points away from the dimerization interface, this results in the interface helix 11 (H11) to remain intact (Figure 3b). This suggests that it should be possible to design improved targeted SERMs for imaging, with larger and stronger paramagnetic or fluorescent groups.

**Orientation of EEu within the LBP.** The structure of the EEu/ER $\alpha$ -LBD complex exhibits the three-layered  $\alpha$ -helical sandwich fold typical of all nuclear receptors (Figure 3a). It is very similar to the structure of the complex of ER $\alpha$ -LBD with the agonist E2 (E2/ER $\alpha$ -LBD, PDB ID 1ERE<sup>10</sup>), with an rms deviation between the two structures of only 0.4 Å over 222 C $\alpha$  atoms. When the two structures are superimposed, the E2 fragments in both structures almost exactly overlap (Figure 4). Moreover, two hydrogen-bonding networks arising from the two hydroxyl groups of the E2 cores are virtually identical in the EEu/ER $\alpha$ -LBD and in the E2/ER $\alpha$ -LBD structure. The phenolic hydroxyl group of EEu (Figures 3b and 4) makes H-bonds with the carboxylate of Glu353, the guanidine of Arg394, the main chain carbonyl of Leu387, and with a conserved water molecule. The 17- $\beta$  hydroxyl group of EEu makes a single hydrogen bond with His524. The H-bonds are thought to provide the majority of the binding free energy for E2.<sup>35</sup> Together with the hydrophobic residues of the binding cavity, they determine the orientation of the steroid ring of E2 or of EEu within the LBP and help to stabilize its “floppy” structure. Because europium ions can contribute a large anomalous

component to X-ray scattering when present and ordered in a protein crystal, we used the anomalous signal to confirm the existence and position of the  $\text{Eu}^{3+}$  in the ligand EEu (Figure 4).

Analogously to other SERMs, such as 4-hydroxytamoxifen (OHT) and raloxifene, EEu is characterized by a steroid core with an extended "side chain" that is thought to be the key factor in making it an antagonist (Figure 1). However, because of the chirality of carbon atom, C17, of the E2 moiety, and to the rigid triple-bond linking it with the Eu-tagged moiety, the orientation of the organometallic moiety is also fixed within the LBP, being almost perpendicular to the flat face of E2, and pointing not toward H12, but in the opposite direction, toward H7 (Figures 3b and 4). As a consequence, H12 is maintained in an "agonist" conformation despite the fact that the Eu tag is much larger than the corresponding moieties of other SERMs, such as OHT. These structural data explain why the EPTA-Lns act as agonists to activate the transcriptional function of  $\text{ER}\alpha$  in breast cancer cells.<sup>5</sup> Similar structural considerations may hold for the binding affinity and agonist activity of novel lanthanide chelates of progesterone interacting with the progesterone receptor.<sup>9</sup>

**Open Conformation of  $\text{ER}\alpha$ -LBD Induced by the Ligand.** The Eu-tagged moiety of EEu juts  $\sim 10$  Å out of the E2 surface, pointing toward H7, and taking over the region occupied in the native receptor by the two-turn helix, H7 (residues 412–417) and by the L7–8 loop (residues 418–421) between H7 and H8 (Figures 4 and 5a). The electron density of this region is very weak, making it difficult to model it. It appears as if this part of the structure is pushed away from the LBP by the extruded Eu-tagged fragment and is disordered. Recently, it has been shown that if a phenylvinyl moiety is added at the  $17\alpha$ -position of E2, H7 is deformed into an extended loop, thus increasing the volume of the LBP by 40%.<sup>16</sup> All of this structural information suggests that H7 of LBD may act as a gate permitting or denying access to the LBP.

**Structural Comparison Suggests a New Ligand-Binding Model.** Superposition of the three structures of  $\text{ER}\alpha$ -LBD, complexed with E2, OHT, and EEu, shows that they overlap well in the upper portion of the domain but differ significantly in its lower portion (Figure 5a). On the basis of a comparison of their C $\alpha$  traces, it can be seen that three distinct regions in the lower portion of the LBD (H3, together with the " $\omega$ -loop", H7–H8, and H11, together with loop L11–12), function as a concerted clamp, which locks the ligand in place (Figure 5a). They display different synergistic reciprocating movements, depending on the specific nature of the ligand bound. Upon binding of E2, this "clamp" tightens to form a stable conformation of the LBP via a group of H-bonds generated between the  $17\beta$  hydroxyl group of E2, His524 and Lys531 of H11, Glu419 of H7, and Glu339 of H3 (Figure 5b).<sup>36</sup> In the EEu/ $\text{ER}\alpha$ -LBD complex (Figure 5c), although the estradiol moiety of EEu stabilizes H11 via the H-bond with His524, the bulky Eu tag disrupts the conformation of helix H7 and shortens the helix H3 and H8 by one turn, resulting in an open conformation of the "clamp". In the OHT/ $\text{ER}\alpha$ -LBD complex (Figure 5d), because of the absence of an H-bond between His524 and OHT,<sup>13</sup> binding of OHT cannot stabilize the three elements of the pocket, which, accordingly, display relatively high flexibility as indicated by their B factors. The position of residues 418–423 (H8) in the OHT complex, especially of Glu419, which moves toward both H3 and H11, may cause the conformational changes seen in both H3 and H11 (as indicated by the red arrows in Figure 5a). On the basis of the conformational changes and movements produced by the three ligands in the

motifs forming the LBP,<sup>11</sup> it is suggested that a channel permitting ligands to move in and out of the LBP may be associated with the cavity formed by helices H3, H7–H8, and H11 (perpendicular to the plane of the representation in Figure 5a).

In conclusion, the crystal structure of the EEu/ $\text{ER}\alpha$ -LBD complex provides a blueprint for the design of novel chimeric ligands targeting ER-positive cells. Such estrogenic or antiestrogenic derivatives, synthesized as a hybrid with one or more functional groups, may be used for the diagnosis and treatment of diseases associated with ERs.

## AUTHOR INFORMATION

### Corresponding Author

\*Tel: +972-8-934-4531. Fax: +972-8-934-6312. E-mail: Joel.Sussman@weizmann.ac.il.

## ACKNOWLEDGMENT

We thank Dr. Dalia Seger for help in cloning the plasmid of  $\text{ER}\alpha$ -LBD and Dr. Gordon Leonard (beamline ID29 at the ESRF) for his support in the collection of X-ray data. We thank Dr. Irena Efremenko for help in generating the Gaussian model of EPTA-Eu. We also thank Prof. Israel Silman for his critical comments during preparation of this manuscript. This study was supported by a grant from the Divadol Foundation (to J.L.S.) and by the NIH Grant CA422238 (to H.D.). J.L.S. is the Morton and Gladys Pickman Professor of Structural Biology, H.D. is the incumbent of the Fred and Andrea Fallek Professorial Chair for Breast Cancer Research, and D.M. is the Israel Matz Professor of Organic Chemistry.

## ABBREVIATIONS USED

ER, estrogen receptor; LBD, ligand-binding domain; E2,  $17\beta$ -estradiol; OHT, 4-hydroxytamoxifen; EPTA-Eu, estradiol-pyridine tetra acetate europium; SERM, selective estrogen receptor modulator; SERD, selective estrogen receptor down-regulator

## REFERENCES

- (1) Deroo, B. J.; Korach, K. S. Estrogen receptors and human disease. *J. Clin. Invest.* **2006**, *116*, 561–570.
- (2) Heldring, N.; Pike, A.; Andersson, S.; Matthews, J.; Cheng, G.; Hartman, J.; Tujague, M.; Strom, A.; Treuter, E.; Warner, M.; Gustafsson, J. A. Estrogen receptors: How do they signal and what are their targets. *Physiol. Rev.* **2007**, *87*, 905–931.
- (3) McDonnell, D. P.; Ching-Yi, C.; John, D. N. Capitalizing on the Complexities of Estrogen Receptor Pharmacology in the Quest for the Perfect SERM. *Ann. N. Y. Acad. Sci.* **2001**, *949*, 16–35.
- (4) Ott, I.; Gust, R. Preclinical and clinical studies on the use of platinum complexes for breast cancer treatment. *Anticancer Agents Med. Chem.* **2007**, *7*, 95–110.
- (5) Gunanathan, C.; Pais, A.; Furman-Haran, E.; Seger, D.; Eyal, E.; Mukhopadhyay, S.; Ben-David, Y.; Leitun, G.; Cohen, H.; Vilan, A.; Degani, H.; Milstein, D. Water-soluble contrast agents targeted at the estrogen receptor for molecular magnetic resonance imaging. *Bioconjugate Chem.* **2007**, *18*, 1361–1365.
- (6) Pike, A. C.; Brzozowski, A. M.; Walton, J.; Hubbard, R. E.; Thorsell, A. G.; Li, Y. L.; Gustafsson, J. A.; Carlquist, M. Structural insights into the mode of action of a pure antiestrogen. *Structure* **2001**, *9*, 145–153.
- (7) el Amouri, H.; Vessieres, A.; Vichard, D.; Top, S.; Gruselle, M.; Jaouen, G. Syntheses and affinities of novel organometallic-labeled

estradiol derivatives: a structure-affinity relationship. *J. Med. Chem.* **1992**, *35*, 3130–3135.

(8) Gabano, E.; Cassino, C.; Bonetti, S.; Prandi, C.; Colangelo, D.; Ghiglia, A.; Osella, D. Synthesis and characterisation of estrogenic carriers for cytotoxic Pt(II) fragments: biological activity of the resulting complexes. *Org. Biomol. Chem.* **2005**, *3*, 3531–3539.

(9) Lee, J.; Burdette, J. E.; MacRenaris, K. W.; Mustafi, D.; Woodruff, T. K.; Meade, T. J. Rational Design, Synthesis, and Biological Evaluation of Progesterone-Modified MRI Contrast Agents. *Chem. Biol.* **2007**, *14*, 824–834.

(10) Brzozowski, A. M.; Pike, A. C.; Dauter, Z.; Hubbard, R. E.; Bonn, T.; Engstrom, O.; Ohman, L. G. G. L.; Gustafsson, J. A.; Carlquist, M. Molecular basis of agonism and antagonism in the oestrogen receptor. *Nature* **1997**, *389*, 753–758.

(11) Gee, A. C.; Katzenellenbogen, J. A. Probing conformational changes in the estrogen receptor: evidence for a partially unfolded intermediate facilitating ligand binding and release. *Mol. Endocrinol.* **2001**, *15*, 421–428.

(12) Tamrazi, A.; Carlson, K. E.; Katzenellenbogen, J. A. Molecular sensors of estrogen receptor conformations and dynamics. *Mol. Endocrinol.* **2003**, *17*, 2593–2602.

(13) Shiau, A. K.; Barstad, D.; Loria, P. M.; Cheng, L.; Kushner, P. J.; Agard, D. A.; Greene, G. L. The structural basis of estrogen receptor/coactivator recognition and the antagonism of this interaction by tamoxifen. *Cell* **1998**, *95*, 927–937.

(14) Heldring, N.; Pawson, T.; McDonnell, D.; Treuter, E.; Gustafsson, J. A.; Pike, A. C. Structural insights into corepressor recognition by antagonist-bound estrogen receptors. *J. Biol. Chem.* **2007**, *282*, 10449–10455.

(15) Egner, U.; Heinrich, N.; Ruff, M.; Gangloff, M.; Mueller-Fahrnow, A.; Wurtz, J. M. Different ligands-different receptor conformations: Modeling of the hER alpha LBD in complex with agonists and antagonists. *Med. Res. Rev.* **2001**, *21*, 523–539.

(16) Nettles, K. W.; Bruning, J. B.; Gil, G.; O'Neill, E. E.; Nowak, J.; Guo, Y.; Kim, Y.; DeSombre, E. R.; Dilis, R.; Hanson, R. N.; Joachimiak, A.; Greene, G. L. Structural plasticity in the oestrogen receptor ligand-binding domain. *EMBO Rep.* **2007**, *8*, 563–568.

(17) Suino-Powell, K.; Xu, Y.; Zhang, C.; Tao, Y. G.; Tolbert, W. D.; Simons, S. S., Jr.; Xu, H. E. Doubling the size of the glucocorticoid receptor ligand binding pocket by deacylcortivazol. *Mol. Cell. Biol.* **2008**, *28*, 1915–1923.

(18) Chrencik, J. E.; Orans, J.; Moore, L. B.; Xue, Y.; Peng, L.; Collins, J. L.; Wisely, G. B.; Lambert, M. H.; Kliewer, S. A.; Redinbo, M. R. Structural disorder in the complex of human pregnane X receptor and the macrolide antibiotic rifampicin. *Mol. Endocrinol.* **2005**, *19*, 1125–1134.

(19) Celik, L.; Lund, J. D.; Schiott, B. Conformational dynamics of the estrogen receptor alpha: molecular dynamics simulations of the influence of binding site structure on protein dynamics. *Biochemistry* **2007**, *46*, 1743–1758.

(20) Sonoda, M. T.; Martinez, L.; Webb, P.; Skaf, M. S.; Polikarpov, I. Ligand dissociation from estrogen receptor is mediated by receptor dimerization: Evidence from molecular dynamics simulations. *Mol. Endocrinol.* **2008**, *22*, 1565–1578.

(21) Shen, J.; Li, W.; Liu, G.; Tang, Y.; Jiang, H. Computational Insights into the Mechanism of Ligand Unbinding and Selectivity of Estrogen Receptors. *J. Phys. Chem. B* **2009**, *113*, 10436–10444.

(22) Burendahl, S.; Danciulescu, C.; Nilsson, L. Ligand unbinding from the estrogen receptor: A computational study of pathways and ligand specificity. *Proteins* **2009**, *77*, 842–856.

(23) Hegy, G. B.; Shackleton, C. H.; Carlquist, M.; Bonn, T.; Engstrom, O.; Sjöholm, P.; Witkowska, H. E. Carboxymethylation of the human estrogen receptor ligand-binding domain-estradiol complex: HPLC/ESMS peptide mapping shows that cysteine 447 does not react with iodoacetic acid. *Steroids* **1996**, *61*, 367–373.

(24) Leduc, A. M.; Trent, J. O.; Wittliff, J. L.; Bramlett, K. S.; Briggs, S. L.; Chirgadze, N. Y.; Wang, Y.; Burris, T. P.; Spatola, A. F. Helix-stabilized cyclic peptides as selective inhibitors of steroid

receptor-coactivator interactions. *Proc. Natl. Acad. Sci. U.S.A.* **2003**, *100*, 11273–11278.

(25) Goldstein, S. W.; Bordner, J.; Hoth, L. R.; Geoghegan, K. F. Chemical and biochemical issues related to X-ray crystallography of the ligand-binding domain of estrogen receptor alpha. *Bioconjugate Chem.* **2001**, *12*, 406–413.

(26) McPherson, A.; Cudney, B. Searching for silver bullets: An alternative strategy for crystallizing macromolecules. *J. Struct. Biol.* **2006**, *156*, 387–406.

(27) Otwinowski, Z.; Minor, W. Processing of X-ray Diffraction Data Collected in Oscillation Mode. *Methods Enzymol.* **1997**, *276*, 307–326.

(28) McCoy, A. J. Solving structures of protein complexes by molecular replacement with Phaser. *Acta Crystallogr., Sect. D: Biol. Crystallogr.* **2007**, *63*, 32–41.

(29) The CCP4 suite: Programs for protein crystallography. *Acta Crystallogr., Sect. D: Biol. Crystallogr.* **1994**, *50*, 760–763.

(30) Moriarty, N. W.; Grosse-Kunstleve, R. W.; Adams, P. D. electronic Ligand Builder and Optimization Workbench (eLBOW): A tool for ligand coordinate and restraint generation. *Acta Crystallogr., Sect. D: Biol. Crystallogr.* **2009**, *65*, 1074–1080.

(31) Adams, P. D.; Afonine, P. V.; Bunkoczi, G.; Chen, V. B.; Davis, I. W.; Echols, N.; Headd, J. J.; Hung, L.-W.; Kapral, G. J.; Grosse-Kunstleve, R. W.; McCoy, A. J.; Moriarty, N. W.; Oeffner, R.; Read, R. J.; Richardson, D. C.; Richardson, J. S.; Terwilliger, T. C.; Zwart, P. H. PHENIX: A comprehensive Python-based system for macromolecular structure solution. *Acta Crystallogr., Sect. D: Biol. Crystallogr.* **2010**, *66*, 213–221.

(32) Emsley, P.; Cowtan, K. Coot: Model-building tools for molecular graphics. *Acta Crystallogr., Sect. D: Biol. Crystallogr.* **2004**, *60*, 2126–2132.

(33) Painter, J.; Merritt, E. A. Optimal description of a protein structure in terms of multiple groups undergoing TLS motion. *Acta Crystallogr., Sect. D: Biol. Crystallogr.* **2006**, *62*, 439–450.

(34) Chen, V. B.; Arendall, W. B., III; Headd, J. J.; Keedy, D. A.; Immormino, R. M.; Kapral, G. J.; Murray, L. W.; Richardson, J. S.; Richardson, D. C. MolProbity: All-atom structure validation for macromolecular crystallography. *Acta Crystallogr., Sect. D: Biol. Crystallogr.* **2010**, *66*, 12–21.

(35) Anstead, G. M.; Carlson, K. E.; Katzenellenbogen, J. A. The estradiol pharmacophore: Ligand structure-estrogen receptor binding affinity relationships and a model for the receptor binding site. *Steroids* **1997**, *62*, 268–303.

(36) Gangloff, M.; Ruff, M.; Eiler, S.; Duclaud, S.; Wurtz, J. M.; Moras, D. Crystal structure of a mutant hERalpha ligand-binding domain reveals key structural features for the mechanism of partial agonism. *J. Biol. Chem.* **2001**, *276*, 15059–15065.